

## Supplemental Material

for

### Lanthanum Nitride $\text{LaN}_9$ Featuring Azide Units: the First Metal Nine-nitride as High-energy Density Material

Shuyi Lin<sup>1,2,#</sup>, Jingyan Chen<sup>1,#</sup>, Bi Zhang<sup>1</sup>, Jian Hao<sup>1,\*</sup>, Meiling Xu<sup>1,\*</sup> and Yinwei Li<sup>1</sup>

<sup>1</sup>Laboratory of Quantum Functional Materials Design and Application, School of Physics and  
Electronic Engineering, Jiangsu Normal University, Xuzhou 221116, China

<sup>2</sup>Department of Applied Physics, The Hong Kong Polytechnic University, Hunghom, Hong Kong,  
China

Corresponding authors: xml@calypso.cn and jian\_hao@jsnu.edu.cn

#### A New High-Pressure Phase for $\text{LaN}_4$

In addition to the known La-N compounds, and newly predicted  $\text{LaN}_9$ , a notable monoclinic phase for  $\text{LaN}_4$  (denoted as *P*-1  $\text{LaN}_4$ ), in the pressure range from 39 to 83 GPa is predicted. Combined with previous reports<sup>1</sup>,  $\text{LaN}_4$  is energetically stable above 14 GPa, then undergoes a structural transition from *C2/c* to *P*-1 structure at 39 GPa, and finally it decomposes into *C2/c*  $\text{LaN}_3$  and *Cm*  $\text{LaN}_8$  at 83 GPa. As shown in Fig. S4(b), *P*-1  $\text{LaN}_4$  possesses  $\text{N}_4$  chair-type polymeric nitrogen units with an average N-N bond length of 1.33 Å at 50 GPa. Figure S4 (c) suggests that the N-N bonding states are fully occupied, while the antibonding states are partially occupied, indicating the covalent bonding between neighboring N atoms. The ICOHP value for N-N in *P*-1  $\text{LaN}_4$  is -4.2, which is smaller in absolute magnitude compared to that of N-N in both  $\text{LaN}_9$  and *Cm*  $\text{LaN}_8$ , indicating the relatively weaker N-N covalent bonding in *P*-1  $\text{LaN}_4$ . Phonon spectra calculations and AIMD simulations demonstrate the dynamical and thermal stability of *P*-1  $\text{LaN}_4$  at 50 GPa [Figs. S5(a) and S5(b)]. Band structure calculation reveals the metallic property of *P*-1  $\text{LaN}_4$  [Fig. S5(c)]. After the structure optimization,  $\text{N}_4$  chair-type polymeric nitrogen units will turn into nitrogen molecules at ambient pressure [Fig. S4(d)], attributed to the weak N-N covalent interactions.

## Families of binary metal nitrides

H																				He
Li	Be											B	C	N	O	F	Ne			
Na	Mg											Al	Si	P	S	Cl	Ar			
K	Ca	Sc	Ti	V	Cr	Mn	Fe	Co	Ni	Cu	Zn	Ga	Ge	As	Se	Br	Kr			
Rb	Sr	Y	Zr	Nb	Mo	Tc	Ru	Rh	Pd	Ag	Cd	In	Sn	Sb	Te	I	Xe			
Cs	Ba		Hf	Ta	W	Re	Os	Ir	Pt	Au	Hg	Tl	Pb	Bi	Po	At	Rn			
Fr	Ra		Rf	Db	Sg	Bh	Hs	Mt	Ds	Rg	Cn		Gd							

La	Ce	Pr	Nd	Pm	Sm	Eu	Gd	Tb	Dy	Ho	Er	Tm	Yb	Lu
Ac	Th	Pa	U	Np	Pu	Am	Cm	Bk	Cf	Es	Fm	Md	No	Lr

- The synthesized or predicted metal nitrides at high pressure
- Unstable metal nitrides at high pressure
- Unexplored metal nitrides at high pressure

Figure. S01. The families of binary metal nitrides at high pressure. Lanthanum, a member of the lanthanide series, tends to have higher production costs compared to other metals such as lithium, sodium, potassium, calcium, magnesium, iron, nickel, and copper. This is primarily attributed to the relative scarcity of lanthanides and the complexity involved in their extraction processes. Despite these higher production costs, it is noteworthy that a high level of purity, specifically 99.99%, can be obtained for lanthanum at a cost of \$3.5 per gram. Therefore, lanthanum can be considered relatively affordable.

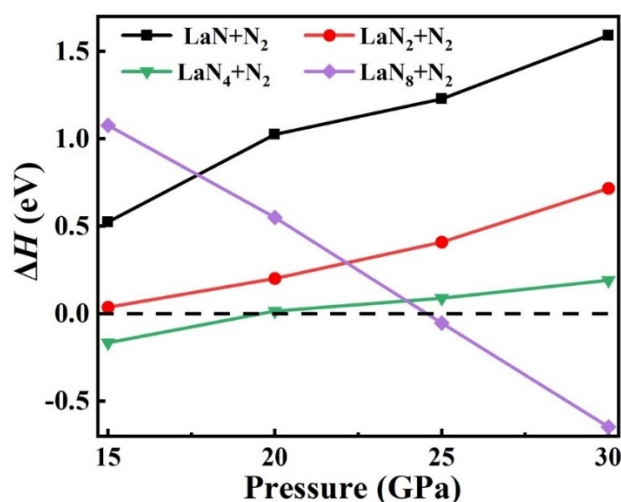


Fig. S1. (a) The formation enthalpy of LaN<sub>9</sub> with respect to decomposition into stable binary compounds and nitrogen at given pressure.

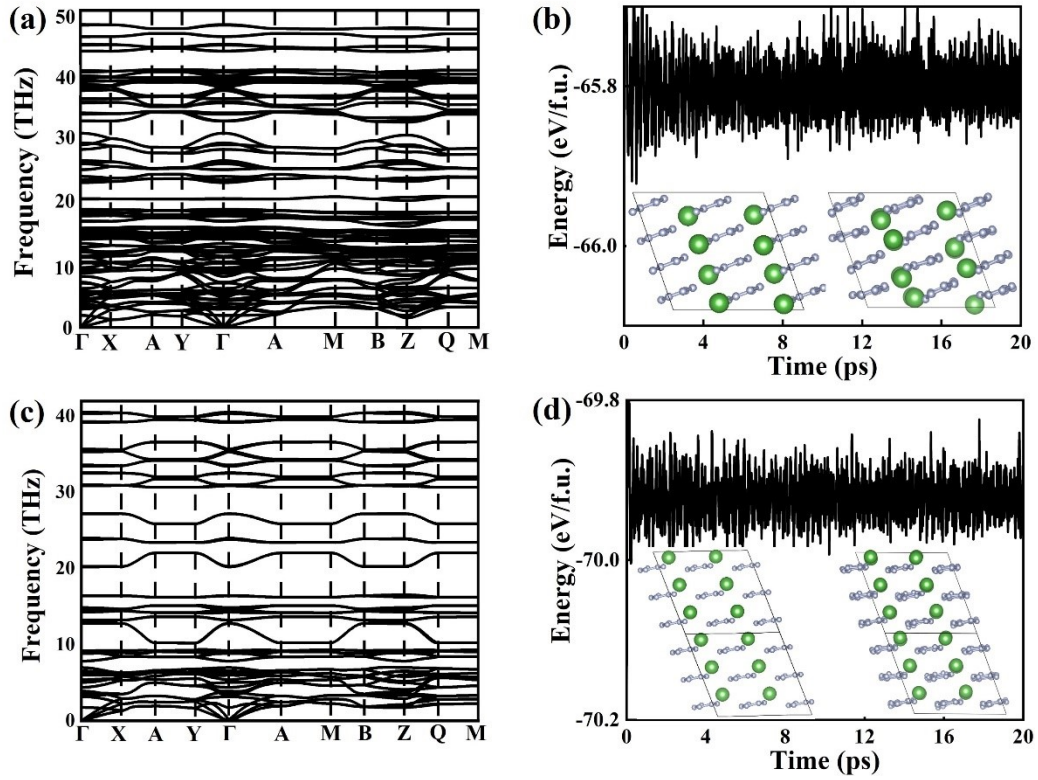


Figure S2. Phonon dispersion curves of LaN<sub>8</sub> at (a) 60 and (c) 0 GPa. Energy fluctuations during MD simulations (300 K) of LaN<sub>8</sub> at (b) 60 and (d) 0 GPa.

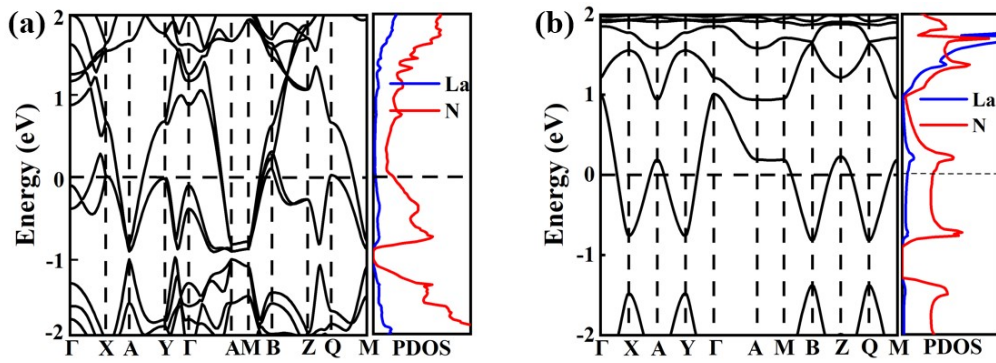


Figure S3. Band structures and PDOS for LaN<sub>8</sub> at (a) 60 GPa and (b) 0 GPa.

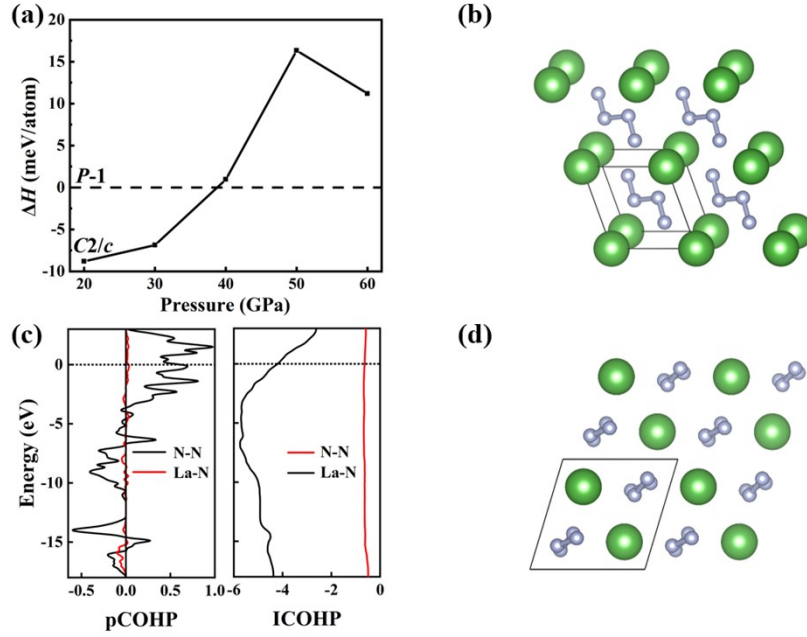


Figure S4. (a) The enthalpy difference curves of  $\text{LaN}_4$  in the  $C2/c$  phase with respect to the  $P-1$  phase. (b) Crystal structure of  $\text{LaN}_4$  at 50 GPa. (c) Plots of pCOHP and ICOHP for  $\text{LaN}_4$  at 50 GPa. (d) Crystal structure of  $\text{LaN}_4$  at 0 GPa.

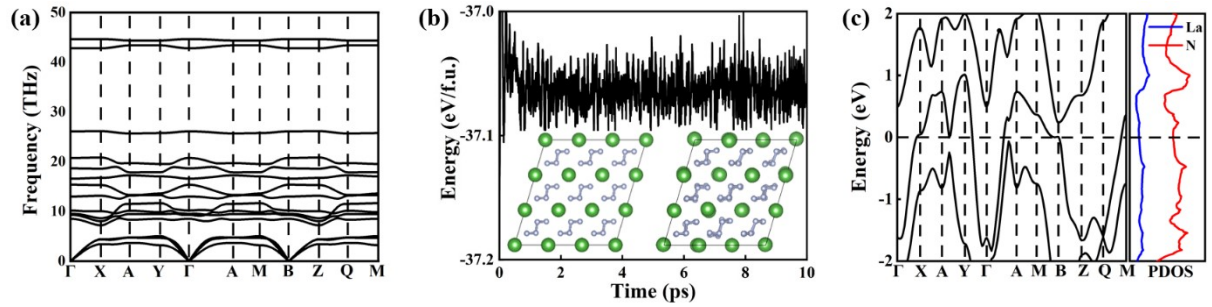


Figure S5. (a) Phonon dispersion curves, (b) energy fluctuations during MD simulations at 300 K, and (c) band structures and PDOS of  $\text{LaN}_4$  at 50 GPa.

Table S01. Common polymerization forms of nitrogen in metal nitrides.

Compounds	Structure type	Nitrogen net
$\text{MN}_3$ (M=Li, Na, K, Rb, Cs), $\text{BaN}_6$ , $\text{Ba}_2\text{N}_{11}$	$\text{N}_3$ units	
$\text{MnN}_4$ , $\text{Al}_2\text{N}_7$ , $\text{Na}_2\text{N}_8$ , $\text{Li}_2\text{N}_4$ , $\text{MgN}_4$	$\text{N}_4$ rings	
$\text{MN}_5$ (M=Li, Na, K, Rb, Cs, Ca, Sr, Ba, Cu, Ta), $\text{MN}_{10}$ (M=Be, Mg, Ba), $\text{MN}_{15}$ (M=Al, Ga, Sc, Y), $\text{HfN}_{20}$	$\text{N}_5$ rings	
$\text{WN}_6$ , $\text{SnN}_6$ , $\text{MN}_3$ (M=Cs, Ca, Sr, K, Mg)	$\text{N}_6$ rings	

MN<sub>4</sub> (M = Be, Cd, Fe, Gd, Re, Os, W, Ru,  
Zn, Sn), GdN<sub>6</sub>, ReN<sub>8</sub>, HfN<sub>10</sub>, ScN<sub>5</sub>, SnN<sub>8</sub>,  
FeN<sub>6</sub>, FeN<sub>4</sub>, FeN<sub>8</sub>, Fe<sub>3</sub>N<sub>8</sub>

N-chains



Table SI. The optimized structural parameters of LaN<sub>4</sub>, LaN<sub>8</sub> and LaN<sub>9</sub>.

Compound	Pressure (GPa)	Space group	$a, b, c$ (Å) $\alpha, \beta, \gamma$ (deg)	Atomic position
LaN <sub>4</sub>	50	<i>P</i> -1	$a=6.366$	La (2a) (0.000, 0.000, 0.000)
			$b=7.034$	N1 (2i) (0.279, 0.739, 0.670)
			$c=5.116$	N2 (2i) (0.551, 0.526, 0.342)
			$\alpha=\gamma=90$	
			$\beta=110.410$	
LaN <sub>8</sub>	0	<i>Cm</i>	$a=6.366$	La(2a) (1.179, 0.000, 0.283)
			$b=7.034$	N1(4b) (1.257, 0.154, 0.583)
			$c=9.456$	N2(4b) (1.198, -0.171, 0.972)
			$\alpha=\gamma=90$	N3(4b) (0.878, -0.178, 0.696)
			$\beta=149.532$	N4(2a) (0.326, 0.000, 0.094)
				N5(2a) (1.462, 0.000, 0.751)
				La1(2a) (-0.384, 0.000, 0.207)
				La2(2a) (-0.846, 0.000, 0.817)
				N1(4b) (-0.191, -0.162, -0.172)
				N2(4b) (-0.742, -0.161, 0.324)
				N3(4b) (-0.034, -0.825, -0.705)
LaN <sub>8</sub>	50	<i>Cm</i>	$a=9.274$	N4(4b) (-0.481, -0.823, -0.240)
			$b=6.629$	N5(4b) (-0.124, -0.327, -0.195)
			$c=4.605$	N6(4b) (-0.674, -0.329, 0.329)
			$\alpha=\gamma=90$	N7(2a) (-0.414, 0.000, -0.285)
			$\beta=80.883$	N8(2a) (-0.970, 0.000, 0.325)
				N9(2a) (-0.108, 0.000, -0.183)
				N10(2a) (-0.657, 0.000, 0.304)
				La (1b) (0.500, 0.500, 0.500)
				N1(3d) (0.000, 0.000, 0.500)
				N2(6g) (0.753, 0.500, 0.000)
LaN <sub>9</sub>	20	<i>Pm</i> -3	$a=b=c=4.732$ $\alpha=\beta=\gamma=90$	

Table SII. The calculated elastic constants  $C_{ij}$  (GPa) of LaN<sub>8</sub> and LaN<sub>9</sub> at ambient pressure.

Compounds	$C_{11}$	$C_{12}$	$C_{13}$	$C_{15}$	$C_{22}$	$C_{23}$	$C_{25}$	$C_{33}$	$C_{35}$	$C_{44}$	$C_{46}$	$C_{55}$	$C_{66}$
LaN <sub>8</sub>	55	37	41	-5	317	32	-12	184	-1	31	-2	23	12
LaN <sub>9</sub>	155	25	/	/	/	/	/	/	/	15			

Table SIII. Bader charges analysis of *P*-1 LaN<sub>4</sub>, *cm* LaN<sub>8</sub>, and LaN<sub>9</sub> at high pressure.

Compounds	Pressure	La( $\epsilon$ )	N( $\epsilon$ )
LaN <sub>4</sub>	50	-1.88	+0.47
LaN <sub>8</sub>	60	-1.98	+0.25
LaN <sub>9</sub>	20	-2.10	+0.23

## REFERENCES

- 1 X. Li, X. Zhang, Z. Yang, Y. Liu and G. Yang, Pressure-stabilized graphene-like P layer in superconducting LaP<sub>2</sub>, *Phys. Chem. Chem. Phys.*, 2022, **24**, 6469–6475.